in dispersion attributable to air-density perturbations, which become severe during the final months in orbit. Despite being negative, the results of these attempts were thus in good accord with expectations. There can be little doubt that the dipoles reentered the dense lower atmosphere during a period of several months, centering about the predicted reentry date of 1 January 1966 for the average dipole.

Unfortunately, New Year's celebrations were not punctuated by a display of tiny fireballs. Calculations show that because of their high A/M value and shallow reentry angle, the dipoles were able to radiate heat rapidly enough to avoid disintegration (*7*), and most probably floated back to Earth essentially unharmed. Even had they disintegrated during reentry, the dipoles would have produced trails far too faint to have been visible.

What is the probability of finding a dipole? Since the spread in orbital lifetimes is long, in comparison with 24 hours, the dipoles were distributed almost uniformly along each latitude circle; their density per unit surface area should therefore be greatest in the polar regions. A simple calculation (*7*) demonstrates that the maximum macroscopic surface density is about 5 dipole/km$^2$. Search of a sufficiently large area (and depth of snow) to ensure a probability of 0.9 of recovering at least one dipole in the arctic is feasible, but expensive (*21*). However, no funds were solicited for such a recovery operation.

This report on the fate of the dipoles is intended to be the last. Our gratification at having seen experimental results in agreement with predictions is tempered by the realization that little can be done to clear the clouded reputation of Project West Ford. For, as was observed long ago, the (alleged) evil that projects do lives after them; the good is oft interred with their bones. So let it be with West Ford.

IRWIN I. SHAPIRO

*Lincoln Laboratory, Massachusetts Institute of Technology, Lexington*

### References and Notes

1. C. F. J. Overhage, W. H. Radford, *Proc. IEEE (Inst. Elec. Engrs.)* **52**, 452 (1964).
2. Each dipole was 1.78 cm in length and 0.00178 cm in diameter; the ensemble was placed in a nearly circular, nearly polar orbit at an altitude of about 3650 km. The combined mass of all dipoles was only 20 kg.
3. The first attempted experiment in October 1961 was unsuccessful because the dipoles did not separate individually [P. Waldron, D. C. MacLellan, M. C. Crocker, *Proc. IEEE (Inst. Elec. Engrs.)* **52**, 571 (1964)].
4. W. E. Morrow and D. C. MacLellan, *Astron. J.* **66**, 107 (1961).
5. J. W. Findlay, *Proc. IEEE (Inst. Elec. Engrs.)* **52**, 455 (1964).
6. W. E. Liller, *Science* **143**, 437 (1964).
7. I. I. Shapiro, H. M. Jones, C. W. Perkins, *Proc. IEEE (Inst. Elec. Engrs.)* **52**, 469 (1964); I. I. Shapiro and H. M. Jones, *Science* **134**, 973 (1961).
8. A. R. Sandage and C. Kowal, *Science* **141**, 797 (1963).
9. W. G. Tifft, W. M. Sinton, J. B. Priser, A. A. Hoag, *ibid.*, p. 798.
10. I. L. Lebow, P. R. Drouilhet, N. L. Daggett, J. N. Harris, F. Nagy, *Proc. IEEE (Inst. Elec. Engrs.)* **52**, 543 (1964).
11. *Ibid.*, Special Issue on Project West Ford **52**, No. 5, (1964).
12. F. E. Heart, D. Karp, A. A. Mathiasen, F. Nagy, W. R. Crowther, W. B. Smith, *Proc. IEEE (Inst. Elec. Engrs.)* **52**, 519 (1964).
13. D. C. MacLellan, W. E. Morrow, I. I. Shapiro, *ibid.*, p. 564.
14. L. G. Kraft and J. C. Henry, private communication.
15. D. Karp, private communication.
16. As discussed in reference 7, the double-peak nature of the dipole density distribution, most pronounced at perigee and apogee (Fig. 2), is most likely the result of the manner in which the dipoles separated from their dispenser.
17. The decreases in perigee height and mean altitude are attributable almost exclusively to the effects of sunlight pressure and air drag, respectively; the contribution of charge drag is negligible [I. I. Shapiro, *J. Geophys. Res.* **69**, 4693 (1964)].
18. One might think that since the dipole density is greatest at the semilatus rectum points, signal-to-noise considerations would allow contours to be made there much later than at, say, apogee or perigee. However, the enhancement does not vary simply as the ratio of the densities, because the velocity (hence, the Doppler) spread is widest at the semilatus rectum points. (Differences in range are not too important because the increase with range of the number of dipoles in the common volume of the two antenna beams nearly compensates the inverse fourth power range dependence of the echo strength of a given target.)
19. Since the densities depended on where along the belt the measurements were made, a smooth average curve is also shown in the figure.
20. The final communication experiment between Camp Parks and Westford involved one teletype channel and was performed on 9 April 1964 after the density had decreased by a factor of nearly 10$^3$. A 40-kw transmitter was used, and about 52 words per minute were sent over this channel from the West Coast to the East Coast.
21. E. Fireman, private communication.
22. I thank D. Karp for making, collating, and explaining all *X*-band observations of the dipoles, and L. G. Kraft for preparing the *L*-band observations. Lincoln Laboratory is operated with support from the U.S. Air Force.

29 June 1966

## Deep-Sea Pleistocene Biostratigraphy

Abstract. *The first detailed paleontological analysis of a deep-sea pistoncore from the Caribbean Sea has been completed. The core, P6304-8, was raised from 3927 meters, east of Beata Ridge at 14°59′N, 69°20′W. Formerly, stratigraphic works in this area were based on studies of paleotemperature, measured by the oxygen isotope mass spectrometry method, or on micropaleontological analysis by means of rapid or cursory examinations. For core P6304-8, samples for foraminiferal analysis were taken at 10-centimeter intervals and split into smaller samples containing an average of 710 individuals (smallest sample, 517 individuals); all individuals were then identified and counted. By use of data derived from populations of this size, a statistical reliability was insured within a 5 percent limit. Temperature oscillations, the best method of portraying Pleistocene stratigraphy, were shown by using ratios of the relative abundances of tropical and subtropical planktonic foraminifera to those found in temperate and cooler waters. These ratios correlate well with existing paleotemperature measurements for the same core, obtained by the oxygen isotope mass spectrometry method.*

World-wide climatic fluctuations caused by Pleistocene glaciation are well documented by both terrestrial and marine geological evidence (*1*). Land evidence includes soil horizons, tills, moraines, pollen, and mammalian successions. In the marine environment, Pleistocene stratigraphy has been based

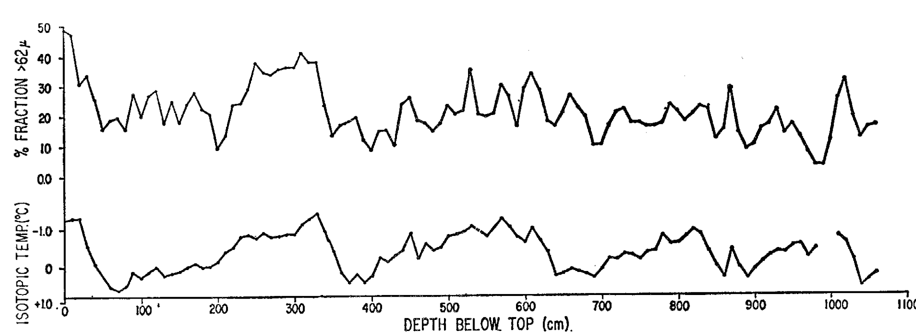


Fig. 1. Core P6304-8. O$^{18}$:O$^{16}$ ratios in the pelagic foraminiferal species *Globigerinoides trilobus sacculifer* (Brady) (δ per mil with respect to the Chicago standard PDB-1) and weight percentages of the sediment fraction larger than 62 μ (from Emiliani, 1966).

chiefly on paleotemperature measurements by the oxygen isotope mass spectrometry method (*2–4*) or paleontological analysis of planktonic foraminifera that have settled to the bottom, forming a major component of the sediments of the ocean floor (*5–12*). This report is based on detailed paleontological analysis of the Caribbean deep-sea core P6304-8 (length, 1050 cm; depth of water, 3927 m; location, 14°59′N, 69°20′W) previously analyzed (*4*) by oxygen isotope and coarse fraction methods (Fig. 1) and estimated to contain a sedimentary record of 225,000 years.

Except for the work by Schott (*5*), prior paleontological analyses of deep-sea cores tend to have insufficient statistical reliability. For these analyses two methods were used. The first, used by Ericson and associates (*6*), is a rapid visual analysis of species frequency in large samples taken at 10-cm stratigraphic intervals; but, since the frequencies are only coarsely estimated, this method does not satisfy the requirements of quantitative investigations. The other method is an actual count of only 300 individuals, often at 50-cm stratigraphic intervals (*10*). Because of the small number of specimens counted, a significant statistical error is often introduced.

In order to maintain a 5-percent error on species distribution with the original ecological universe, samples were split to a size that contained an average of 710 individuals (smallest sample, 517 individuals); then all specimens were identified and counted (*13*). From the population data derived from these samples, which were taken at 10-cm stratigraphic intervals, percentages and ratios of the relative abundances of various species were computed.

Foraminiferal species and subspecies (Table 1) used in the paleontological analysis have all been drawn and discussed taxonomically by Ericson (*8*), Phleger *et al.* (*10*), Parker (*11*), Loeblich *et al.* (*14*), and others. In addition to obtaining the percentage of each individual within the total population and the ratios of relative abundances of selected species, error measures were calculated for correlation purposes. Error measure is the optimum measure in percentage of the amount of correlation between two time series with random components: The components are species percentage, ratios of species percentage, and values taken from the isotopic paleotemperature curve, all from the same sampling interval. The values are derived through a series of

Table 1. Error measures for foraminiferal species and subspecies.

| Species | Error measure (*15*) |
|---|---|
| *Candeina nitida* d'Orbigny | 0.1717 |
| *Globigerina digitata* Brady | .0699 |
| *Globigerinoides conglobatus* (Brady) | .2943 |
| *G. helicina* (d'Orbigny) | .4828 |
| *G. pyramidalis* (Vanden Broeck) | .4185 |
| *G. ruber* (d'Orbigny) | .8536 |
| *G. trilobus sacculifer* (Brady) | .6035 |
| *G. trilobus trilobus* (Reuss) | .2770 |
| *Globoquadrina dutertrei* d'Orbigny | .3971 |
| *Globorotalia crassaformis* (Galloway and Wissler) | .2125 |
| *G. hirsuta* (d'Orbigny) | .0512 |
| *G. inflata* (d'Orbigny) | .6638 |
| *G. menardii fimbriata* (Brady) | .5632 |
| *G. menardii flexuosa* (Koch) | .4326 |
| *G. menardii menardii* (d'Orbigny) | .7695 |
| *G. menardii tumida* (Brady) | .3415 |
| *G. scitula* (Brady) | .1851 |
| *G. truncatulinoides* (d'Orbigny) | .1791 |
| *Hastigerina pelagica* (d'Orbigny) | .5430 |
| *Orbulina universa* d'Orbigny | .1782 |
| *Pulleniatina obliquiloculata* (Parker and Jones) | .2398 |
| *Sphaeroidinella dehiscens* (Parker and Jones) | .4396 |

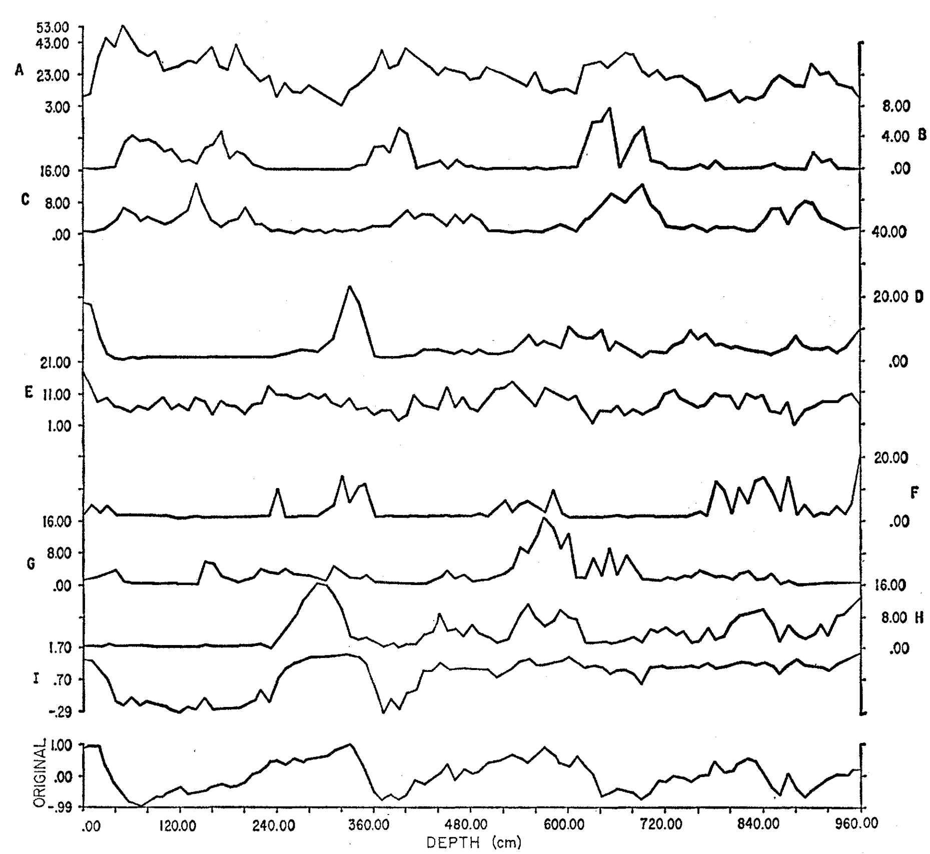


Fig. 2. Core P6304-8. Curves A to I represent relative abundances of planktonic foraminifera percentages. Bottom curve is $O^{18} : O^{16}$ ratio in the pelagic foraminiferal species *Globigerinoides trilobus sacculifer*. (A) *Globigerinoides ruber*; (B) *Globorotalia inflata*; (C) *Hastigerina* complex; (D) *Globorotalia menardii menardii*; (E) *Globigerinoides trilobus sacculifer*; (F) *Pulleniatina obliquiloculata*; (G) *Sphaeroidinella dehiscens*; (H) *Globorotalia menardii flexuosa*; and (I) *Globorotalia menardii* complex (*G. menardii menardii, G. menardii flexuosa, G. menardii tumida, and G. menardii fimbriata*).

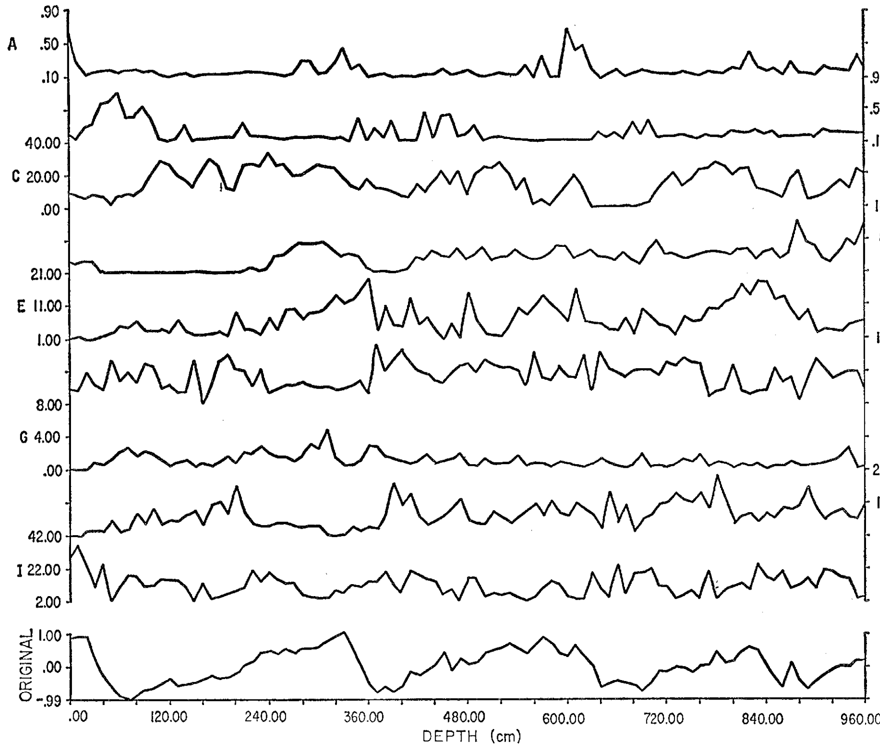


Fig. 3. Core P6304-8. Curves A to I represent relative abundances of planktonic foraminifera percentages. Bottom curve is $O^{18}:O^{16}$ ratio in the pelagic foraminiferal species *Globigerinoides trilobus sacculifer.* (A) *Globorotalia menardii fimbriata*; (B) *Globigerinoides helicina*; (C) *Globoquadrina dutertrei*; (D) *Globorotalia menardii tumida*; (E) *Globigerinoides conglobatus*; (F) *Globigerinoides trilobus trilobus*; (G) *Globorotalia crassaformis*; (H) *Globorotalia truncatulinoides*; and (I) *Orbulina universa.*

mathematical expressions, which are an improvement on classical multiple regression analysis. A complete description of error measure calculation is given by Kemp and Eger (*15*).

Figures 2 and 3 show the relative abundance of the specimens identified and counted, which constitute the major portion of the foraminiferal population. Directly below is a plot of the paleotemperature variations determined by Emiliani (*4*). Some species or groups of species show a well-defined direct correlation with temperature (Fig. 2, lines E, F, G, and H), others show an inverse correlation (Fig. 2, lines A, B, and C), and some show little or no correlation (Fig. 3).

*Globorotalia menardii menardii* displays the best positive correlation with the isotopic temperature curve; *Globigerinoides trilobus sacculifer, Pulleniatina obliquiloculata,* and *Sphaeroidinella dehiscens* also show positive correlation, but to a lesser degree. The "*Globorotalia menardii* group" (*G. menardii menardii, G. menardii tumida, G. menardii flexuosa,* and *G. menardii fimbriata*), used by Ericson and associates (*9*) to delineate Pleistocene temperature oscillations, has been found to be an unreliable indicator of temperature. The major drawback in using the *G. menardii* group is that its specific and subspecific components, some of which are extinct, appear to have considerably different temperature habitats [see Jones (*16*), Bradshaw (*17*), and others]. Thus, by grouping taxa with different paleoecological responses, one may obtain results that sometimes correlate with those obtained by use of more rigorous criteria, but most of the time a random relation appears to exist.

Of further significance in defining high temperature peaks of the paleotemperature curve are the considerable numbers of aberrant forms of planktonic foraminifera. Bradshaw (*18*) and Watabe and Wilber (*19*) have shown in laboratory experiments that certain foraminifera and coccoliths can change their growth trends with changes of only a few degrees above their normal living range. Such occurrences have been noted in bottom sediments by Arnal (*20*), Lidz (*21*), and Watkins (*22*); but their counterparts have not been observed in the water column of the open ocean. Figure 4 illustrates various forms of contortion observed in the species group of *Globorotalia menardii.*

The inverse correlation of *Globigerinoides ruber* with temperature is of striking significance. It is important to note that this species is most abundant in the upper 50 m of the water column and thus is likely to be susceptible to any variation in temperature (*23*). *Globorotalia inflata,* known to be an inhabitant of cool waters, shows trends similar to those of *Globigerinoides ruber.* The same is true for the *Hastigerina-Globigerinella* complex, which previously was thought to be characteristic of warmer waters (*17, 24*), but more recently has been shown to inhabit colder, deeper waters in the equatorial Atlantic (*23*).

Sampling programs of living planktonic foraminifera by Smith (*25*), Bé (*24*), Bradshaw (*17*), Casey (*26*), Enbysk (*27*), Jones (*23*), Lidz (*28*), and others

Table 2. Error measures for species ratios.

| Species ratio | Error measure |
|---|---|
| *Globorotalia menardii menardii, Pulleniatina obliquiloculata,* and *Sphaeroidinella dehiscens* to *Globigerinoides ruber* and *Globorotalia inflata* | 0.8848 |
| *Globorotalia menardii menardii, Pulleniatina obliquiloculata* and *Sphaeroidinella dehiscens* to *Globigerinoides ruber, Globorotalia inflata,* and the *Hastigerina* complex | .8716 |
| *Pulleniatina obliquiloculata* and *Sphaeroidinella dehiscens* to *Globorotalia inflata* | .8021 |
| *Globorotalia menardii menardii* to *Globigerinoides ruber* | .7676 |
| *Globorotalia menardii menardii* to *Globigerinoides ruber* and *Globorotalia inflata* | .7671 |
| *Pulleniatina obliquiloculata* and *Sphaeroidinella dehiscens* to the *Hastigerina* complex | .7429 |
| *Pulleniatina obliquiloculata* and *Sphaeroidinella dehiscens* to *Globigerinoides ruber* and *Globorotalia inflata* | .6399 |
| *Pulleniatina obliquiloculata* and *Sphaeroidinella dehiscens* to *Globigerinoides ruber* | .6254 |
| *Globigerinoides trilobus sacculifer* and *G. trilobus trilobus* to *Globigerinoides ruber* | .6109 |

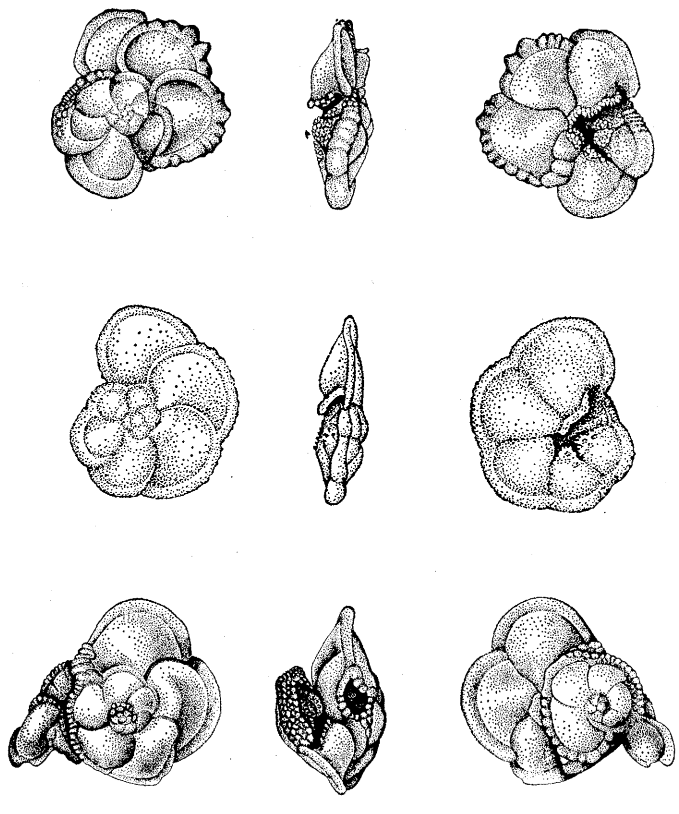

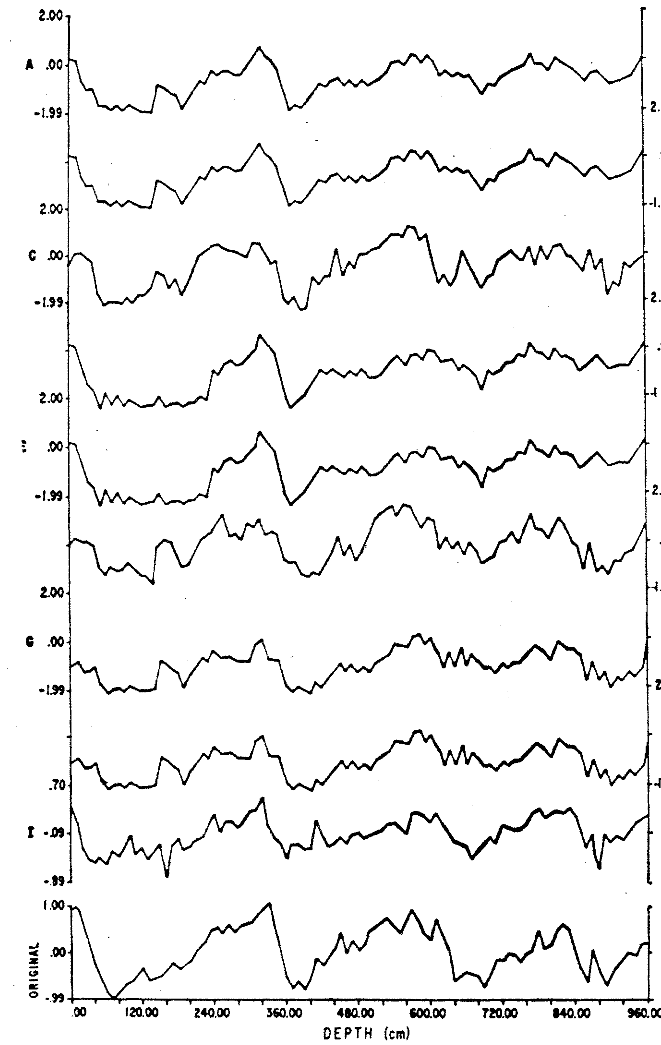


Fig. 4 (left). Top and bottom rows are aberrant forms of *Globorotalia menardii* spp.; middle row is normal forms of *Globorotalia menardii menardii*. Fig. 5 (right). Core P6304-8. Curves A to I represent ratios of the relative abundance of diagnostic stenothermic planktonic foraminiferal species or groups of species. Bottom curve is $O^{18} : O^{16}$ ratio in the pelagic foraminiferal species *Globigerinoides trilobus sacculifer*. (A) *Globorotalia menardii menardii, Pulleniatina obliquiloculata,* and *Sphaeroidinella dehiscens* to *Globigerinoides ruber* and *Globorotalia inflata*; (B) *Globorotalia menardii menardii, Pulleniatina obliquiloculata,* and *Sphaeroidinella dehiscens* to *Globigerinoides ruber, Globorotalia inflata,* and the *Hastigerina* complex; (C) *Pulleniatina obliquiloculata* and *Sphaeroidinella dehiscens* to *Globorotalia inflata*; (D) *Globorotalia menardii menardii* to *Globigerinoides ruber*; (E) *Globorotalia menardii menardii to Globigerinoides ruber* and the *Hastigerina* complex; (F) *Pulleniatina obliquiloculata* and *Sphaeroidinella dehiscens* to *Hastigerina* complex; (G) *Pulleniatina obliquiloculata* and *Sphaeroidinella dehiscens* to the *Hastigerina* complex and *Globigerinoides ruber*; (H) *Pulleniatina obliquiloculata* and *Sphaeroidinella dehiscens* to *Globigerinoides ruber*; and (I) *Globigerinoides trilobus sacculifer* and *G. trilobus trilobus* to *Globigerinoides ruber*.

indicate that certain planktonic foraminifera are restricted to characteristic water temperatures. Percentage analysis of fossil planktonic foraminiferal populations forms a closed statistical system in which the quantities involved are mutually dependent. By using abundance ratios, not only are some of the limitations of the closed system eliminated but also the information is amplified [see Emiliani (*3*)]. For such analysis, species or groups of species that are particularly stenothermic (Table 2) were selected; results are shown in Fig. 5.

The ratios are arranged in order of degree of error measure (*14*). As shown in Table 2, the ratios of *Globorotalia menardii menardii, Pulleniatina obliquiloculata,* and *Sphaeroidinella dehiscens* to *Globigerinoides ruber* and *Globorotalia inflata* and *Globorotalia menardii menardii, P. obliquiloculata,* and *S. dehiscens* to *Globigerinoides ruber, Globorotalia inflata,* and the *Hastigerina-Globigerinella* complex produce error measures of 0.8848 and 0.8716, respectively. These values are improvements over the error measure of *Globigerinoides ruber* (0.8536), the best of all species, and demonstrate the usefulness of using ratios of warm to cool water species. Only three species have error measures better than 0.60 (Table 1), whereas the combination of ratios provides much better values. By comparing Figs. 3 and 6 of Emiliani (*4*), the age of the bottom of core P6304-8 is estimated to be about 225,000 years. The graphs in Figs. 1, 2, 3, and 5 indicate that at least five major temperature minima occurred during this time and that, as shown in this report, ratios of selected planktonic foraminifera can be utilized for accurate biostratigraphic and paleotemperature analysis.

LOUIS LIDZ

*Institute of Marine Science,*
*University of Miami,*
*Miami, Florida 33149*

### References and Notes

1. R. F. Flint, *Glacial and Pleistocene Geology* (Wiley, New York, 1957).
2. C. Emiliani, *J. Geol.* **125**, 538 (1955); *ibid.* **66**, 264 (1958).
3. ———, *Bull. Geol. Soc. Amer.* **75**, 129 (1964).
4. ———, *J. Geol.* **74**, 109 (1966).
5. W. Schott, *Wiss. Ergeb. Deut. Atlan. Exp. "Meteor,"* **III**, T.3, 43 (1935); *Medd. Oceanogr. Inst. Göteborg, Contrib. 18, Ser. B,* **6**, No. 2 (1952).
6. D. B. Ericson, G. Wollin, J. Wollin, *Deep-Sea Res.* **2**, 152 (1954).
7. M. Ewing, D. B. Ericson, B. C. Heezen, in *Habitat of Oil*, L. Weeks, Ed. (Amer. Ass. Petroleum Geologists, Tulsa, 1958), pp. 995–1053.

8. D. B. Ericson, M. Ewing, G. Wollin, B. C. Heezen, *Bull. Geol. Soc. Amer.* **72**, 193 (1961).
9. ———, *Science* **146**, 723 (1964).
10. F. B. Phleger, F. L. Parker, J. F. Peirson, *Rep. Swedish Deep Sea Exp. (1947-1948)* **7**, 1 (1953).
11. F. L. Parker, *ibid.* **8**, No. 4, 219 (1958).
12. R. Todd, *ibid.* **8**, No. 3, 169 (1958).
13. Five-percent error on species distribution is achieved by using an average of 710 specimens per sample and verified by the use of Tchebycheff's theorem [H. Cramer, *The Elements of Probability Theory* (Wiley, New York, 1955), p. 81].
14. A. R. Loeblich, Jr., *et al.*, *U.S. Nat. Mus. Bull. 215* (1957).
15. W. Kemp and D. Eger, *J. Geophys. Res.*, in press. Error measure is the optimum measure in percentage of the amount of correlation between two time series with random components.
16. J. I. Jones, data presented at International Co-operative Investigations of the Tropical Atlantic Symposium, Abidjan, October 1966.
17. J. S. Bradshaw, *Contrib. Cushman Found. Foraminiferal Res.* **10**, 25 (1959).
18. ———, *J. Paleontol.* **31**, 1138 (1957).
19. N. Watabe and K. M. Wilber, *Limnol. Oceanogr.* **11**, 567 (1966).
20. R. E. Arnal, *The Compass* (Sigma Gamma Epsilon Soc.) **32**, 185 (1955).
21. L. Lidz, *Limnol. Oceanogr.* **10**, 392 (1965).
22. J. G. Watkins, *Micropaleontology* **5**, 101 (1959).
23. J. I. Jones, *Bull. Amer. Ass. Petrol. Geol.* **50**, 619 (1966).
24. A. W. H. Bé, *Micropaleontology* **6**, 373 (1960).
25. A. B. Smith, *Contrib. Cushman Found. Foraminiferal Res.* **14**, 1 (1963).
26. R. Casey, *Bull. Amer. Ass. Petrol. Geol.* **47**, 1768 (1963).
27. B. J. Enbysk, *ibid.* **49**, 1760 (1965).
28. L. Lidz, *Limnol. Oceanogr.* **11**, 257 (1966).
29. I thank Barbara Lidz for illustrations of foraminifera, W. Kemp for providing the computer program so that all data in this report could be processed by an I.B.M. 7040 computer, and C. Emiliani for his continued encouragement. Financial support provided by NSF grant GP-5012.
30. Contribution No. 715 from the Institute of Marine Science, University of Miami.

10 October 1966

# Inverse Compton Effect: Some Consequences for Quasars

Abstract. *The inverse Compton effect can transform enough energy of relativistic electrons into radiation so that an upper limit to the mean energy of the electrons is set. In quasars, the limit is too small to allow the production of any appreciable amount of synchrotron or inverse Compton radiation, unless either the distances are not cosmological or the lifetimes of the relativistic electrons are extremely short, of the order of hours.*

The inverse Compton effect increases the energy of photons by collisions of the photons with high-energy electrons. If the energy transfer caused by each collision is too large, then the radiation density and accordingly the Compton losses will grow continuously. This growth is stopped by the breakdown of the energy stored in the relativistic electrons. Thus the mean energy of the electrons is reduced below a critical value; the characteristic time is $< R/c$ ($R$, radius of the quasar). This holds even when energy is continuously resupplied. Therefore, the inverse Compton effect limits the possible mean energy of the relativistic electrons and thus puts restrictions on quasar models.

By $E_e$ (in metric units) and $\gamma_e$ (in units of the rest energy $m_0c^2$ of the electrons) we denote the energy of individual relativistic electrons, while $E$ and $\gamma$ (without subscript) are the mean values averaged over all relativistic electrons.

The total radiation power of an electron of energy $E_e = m_0c^2\gamma_e$ as it is scattered by low-energy photons of radiation density $U$ is (*1*)

$$p_c = 4\, c\, \sigma_0\, \gamma^2\, U/3 \qquad (1)$$

where $\sigma_0 = 6 \cdot 10^{-25}$ cm$^2$, which is the Thompson cross section. If $U$ contains photons of frequencies up to the ultraviolet, the formula is valid for $30 < \gamma_e < 10^4$ and may be used for approximations also with higher values of $\gamma_e$. If we replace the mean radiation power $P_c \equiv p_c\ (\gamma)$ by the corresponding Compton luminosity $L_c = 4\pi R^3 N_c P_c/3$ (which is possible only if $L_c$ is approximately constant within a time of the order of $R/c$), then

$$L_c = 4\, R\sigma_0\, N_e\, \gamma^2\, L/3 \qquad (2)$$

$N_e$ is the number density of relativistic electrons, and $L = 4\pi R^2\ c\, U/3$, the total luminosity. If we write $L = L_t + L_s + L_c$ ($L_t$ denoting a possible thermal component, $L_s$ the synchrotron component), it is obvious from Eq. 2 that the inequality

$$4\, R\sigma_0\, N_e\, \gamma^2/3 \leqq (L_c + L_s)/L \leqq 1 \qquad (3)$$

must hold. As long as the left-hand side is $> 0.5$, the inverse Compton effect, as compared to the synchrotron mechanism and any thermal emission, is dominating.

The mean lifetime of the relativistic electrons, defined as the time in which half of the energy is lost by radiation, is $\tau = E/P$, where $E = m_0\, c^2\, \gamma$ is the mean electron energy, and $P = P_c + P_s$. Here, $P_s$ denotes the mean radiation power due to synchrotron emission.

From Eq. 3 it follows that

$$\gamma \leqq \frac{3(L_c + L_s)}{4\, R\sigma_0\, N_e\, \gamma\, L} = \frac{3}{4\, R\sigma_0\, L\, N_e} \times \frac{4\ \pi R^3\ N_e\ (P_c + P_s)}{3} \cdot \frac{m_0\, c^2}{\tau\ P} = \frac{\pi\, R\, m_0\, c^3}{\sigma_0\, L} \cdot \frac{R}{c\ \tau}$$

$L$ cannot be measured directly but has to be calculated from the observed intensity by means of an assumed photometric distance, $D_a$. If $D$ is the real photometric distance, the actual luminosity differs from the calculated one by a factor $(D/D_a)^2$.

With typical values for quasars: $R = 10^{17}$ cm, $L = 3 \cdot 10^{46}$ erg per second (luminosity calculated from a cosmological interpretation of the red shifts)

$$\gamma \leqq 0.5\ (D/D_a)^{-2}\ (\tau c/R)^{-1} \qquad (5)$$

On the other hand, the fact that nonthermal radiation is emitted by quasars gives a lower limit for $\gamma$. In order that any appreciable amount of synchrotron or inverse Compton radiation be emitted at all, it is necessary that $\gamma > 30$. Furthermore, in order that energy be emitted in a frequency range of several orders of magnitude it is probable that $\gamma$ has a still higher value, at least of the order of $10^2$. It is impossible to give a definite estimate of $\gamma$ without using more detailed characteristics of the radiation spectrum. In any case, the upper limit of $\gamma$ given by Eq. 5 must exceed the lower limit, and therefore at least one of the factors in Eq. 5 should be appreciably larger than unity. In other words, in a "cosmological" quasar model with large electron lifetimes the mean electron energy would be limited by Eq. 5 to an impossibly small value. This conclusion is independent from whether or not the major part of the radiation is due to the inverse Compton effect. So we are left with two possibilities.

The first is that the assumed distances are too large. Terrell's hypothesis (*2*), of a gigantic explosion in the Milky Way some $10^7$ years ago reduces the distance by a factor of about $10^3$. By use of this factor in Eq. 5, it follows that the mean lifetime of the relativistic electrons may be appreciably larger than $R/c$, but should not exceed a few hundred years.

Under the second possibility we assume that the cosmological interpretation of the red shifts is correct. Then it follows that the lifetime of the relativistic electrons must be extremely short, of the order of minutes to hours.